JOURNAL OF VIROLOGY, Apr. 1995, p. 2471–2479 Vol. 69, No. 4
0022-538X/95/$04.00+0

Mutations in the Putative Fusion Peptide of Semliki Forest Virus Affect Spike Protein Oligomerization and Virus Assembly

WAYNE A. DUFFUS, PNINA LEVY-MINTZ,† MATTHEW R. KLIMJACK, AND MARGARET KIELIAN*

Department of Cell Biology, Albert Einstein College of Medicine, Bronx, New York 10461

Received 2 December 1994/Accepted 18 January 1995

The two transmembrane spike protein subunits of Semliki Forest virus (SFV) form a heterodimeric complex in the rough endoplasmic reticulum. This complex is then transported to the plasma membrane, where spike-nucleocapsid binding and virus budding take place. By using an infectious SFV clone, we have characterized the effects of mutations within the putative fusion peptide of the E1 spike subunit on spike protein dimerization and virus assembly. These mutations were previously demonstrated to block spike protein membrane fusion activity (G91D) or cause an acid shift in the pH threshold of fusion (G91A). During infection of BHK cells at 37°C, virus spike proteins containing either mutation were efficiently produced and transported to the plasma membrane, where they associated with the nucleocapsid. However, the assembly of mutant spike proteins into mature virions was severely impaired and a cleaved soluble fragment of E1 was released into the medium. In contrast, incubation of mutant-infected cells at reduced temperature (28°C) dramatically decreased E1 cleavage and permitted assembly of morphologically normal virus particles. Pulse-labeling studies showed that the critical period for 28°C incubation was during virus assembly, not spike protein synthesis. Thus, mutations in the putative fusion peptide of SFV confer a strong and thermoreversible budding defect. The dimerization of the E1 spike protein subunit with E2 was analyzed by using either cells infected with virus mutants or mutant virus particles assembled at 28°C. The altered-assembly phenotype of the G91D and G91A mutants correlated with decreased stability of the E1-E2 dimer.

Enveloped animal viruses use membrane fusion to infect host cells. For a number of enveloped viruses, this key step in the viral infection pathway is triggered by the low pH to which the virus is exposed during its transit through the endocytic pathway of the cell (reviewed in references 2, 29, and 41). Such an endocytic entry pathway was first demonstrated to be the productive route of infection for Semliki Forest virus (SFV), an enveloped alphavirus (13). SFV fusion is mediated by the virus spike protein, which contains two type I integral membrane glycopolypeptides, E1 (50,786 Da) and E2 (51,855 Da), and a peripheral glycopolypeptide, E3 (11,369 Da) (reviewed in references 10, 17, and 37). A variety of evidence indicates that fusion is mediated by the E1 subunit, which contains the putative virus fusion peptide, a highly conserved hydrophobic domain (9, 22). Upon exposure of SFV to low pH, the E1 subunit rapidly converts to an acid conformation that is specifically recognized by a series of monoclonal antibodies (MAbs), is trypsin resistant, and is composed of an oligomer of three E1 subunits (reviewed in reference 17). This acid form of E1 mediates SFV membrane fusion, presumably by an interaction of the E1 ectodomain with the target bilayer.

In addition to their use as a highly developed system to study membrane fusion, alphaviruses such as SFV and Sindbis virus are also useful experimental paradigms for studying the molecular mechanisms of virus biosynthesis, assembly, and budding (reviewed in references 10, 17, and 37). The SFV structural proteins are synthesized as a polyprotein from a subgenomic mRNA and cleaved to form the viral polypeptides. E3 and E2 are initially synthesized as a precursor form termed p62 that is posttranslationally processed after an ArgHisArg Arg sequence, probably in the trans-Golgi network (5). The E1 and p62 subunits associate within the rough endoplasmic reticulum to form noncovalent heterodimers (46) and are transported as a complex through the rough endoplasmic reticulum and Golgi to the plasma membrane. Evidence suggests that this dimerization is required for proper protein transport and folding (21, 22, 31) and that the E3 portion of the p62 subunit may be involved in dimerization with E1 or transport of the polypeptide complex (26, 39). Following arrival at the plasma membrane, the spike proteins interact with the viral nucleocapsid via the E2 cytoplasmic domain to mediate the budding and release of progeny virus particles (27, 38, 44). A short, hydrophobic polypeptide known as 6K is located between p62 and E1 in the polyprotein, associates with the E1-p62 dimer during transport, and appears to play a role in the efficient budding of virus from the cell (23). On the surface of the virus-infected cell and in the assembled virus particle, the heterotrimeric spike protomers are organized into 80 spikes, each one a trimer containing $(E1\text{-}E2\text{-}E3)_3$. Both the nucleocapsid core and the spike protein lattice of the virus are highly ordered and are present as T=4 icosahedra in the virus particle (17, 37).

In previous work, we have described the effects of a number of mutations in the SFV E1 hydrophobic domain on spike protein transport and low-pH-triggered cell-cell fusion activity (22). The putative fusion domain extends from amino acids 75 to 97 of E1 and is largely identical among different alphaviruses. Two mutations in this region had no observed effect on the spike protein (K79Q and M88L), while two less conservative substitutions (P86D and G91P) or a deletion of amino acids 83 to 92 blocked transport of the E1 subunit to the cell surface. A number of mutations had no apparent effect on transport of either E1 or E2 to the plasma membrane but strongly affected spike protein fusion activity (D75A, G83A, G91A, and G91D). Most interestingly, the G91D mutation

* Corresponding author. Mailing address: Department of Cell Biology, Albert Einstein College of Medicine, 1300 Morris Park Ave., Bronx, NY 10461. Phone: (718) 430-3638. Fax: (718) 829-7619. Electronic mail address: kielian@aecom.yu.edu.

† Present address: Division of Infectious Diseases, Thomas Jefferson University, Philadelphia, PA 19107.

completely blocked the ability of the spike protein to carry out low-pH-triggered cell-cell fusion. The conservative G91A mutation at the same position in E1 caused a shift in the pH threshold of fusion from pH 6.5 in the wild type (WT) to ~pH 5.4 in the mutant.

Since these mutagenesis studies were performed on an SFV structural protein clone, the effects of the mutations on virus assembly and infectivity could not be examined. Here we have used an SFV infectious clone (23) to express the G91D and G91A mutations in virus. The mutations were found to confer a strong virus assembly defect that was repressed by incubation at low temperature and correlated with an alteration in the stability of the E1-E2 spike protein dimer.

MATERIALS AND METHODS

Construction of infectious SFV clones containing the WT, G91A, and G91D sequences. Clones of the structural proteins of the G91A and G91D mutants and our WT SFV isolate were previously characterized by using pL2, a late simian virus 40-based expression plasmid (22). To analyze the effects of the G91D and G91A mutations in virus, *Cla*I restriction fragments containing the E1 putative fusion peptide were subcloned into the pSP6-SFV4 infectious SFV clone (23), kindly given to us by Peter Liljeström and Henrik Garoff. To prepare the infectious clone vector for subcloning, pSP6-SFV4 (14,411 bp) was digested to completion with *Cla*I and the 13,776-bp fragment was self-ligated and propagated to yield a plasmid containing all of the WT sequences except the *Cla*I fragment. This plasmid was then linearized with *Cla*I at the single unique site, treated with phosphatase, and ligated to the 635-bp *Cla*I fragments purified from WT and mutant pL2 clones (22) to regenerate the complete infectious clone. The ligation mixtures were transformed into *Escherichia coli* DH5α, and single colonies were screened for acquisition of the insert. Plasmid DNAs were isolated from positive cultures and analyzed by restriction digestion to select clones with the correct orientation of the *Cla*I fragment. In addition, this screening was necessary since in our study, pSP6-SFV4 was somewhat unstable and subject to rearrangement during propagation in bacteria. Two isolates each of WT, G91A, and G91D were characterized to control for possible mutations arising during subcloning; the results obtained with both isolates were identical. These clones will now be referred to as the WT infectious clone (WT-IC), G91A, and G91D. The DNA from 250-ml cultures of each isolate was purified on CsCl gradients or by Qiagen column chromatography (Qiagen, Inc., Chatsworth, Calif.) and used for in vitro transcription.

In vitro transcription of infectious SFV RNA and electroporation into BHK cells. The WT and mutant constructs in plasmid pSP6-SFV were linearized with *Spe*I and used as templates for in vitro transcription. The transcription reaction was performed essentially as previously described (23), with 1 to 1.5 μg of DNA in a 50-μl total reaction volume containing 40 mM *N*-2-hydroxyethylpiperazine-*N*′-2-ethanesulfonic acid (HEPES)-KOH (pH 7.4); 6 mM magnesium acetate; 2 mM spermidine-HCl; 100 μg of acetylated bovine serum albumin (BSA) per ml; 1 mM m7G(5′)ppp(5′)G (New England Biolabs, Beverly, Mass.); 10 mM dithiothreitol; 1 mM each ATP, CTP, and UTP; 0.5 mM GTP; 50 U of RNasin (Promega, Madison, Wis.); and 20 to 50 U of SP6 polymerase (Epicentre Technology, Madison, Wis.) and incubation at 37°C for 60 min. The quantity and quality of RNA production were estimated by electrophoresis of an aliquot of the reaction mixture on a 0.5% agarose gel containing ethidium bromide. The transcription mixture was stored at −70°C for subsequent use.

Electroporation was performed as described by Liljeström et al. (23), with 5×10^6 to 7.5×10^6 BHK-21 cells in 0.5 ml of phosphate-buffered saline (PBS)–3 to 10 μl of the RNA transcription reaction mixture and two pulses at 1.5 kV and 25 μF on a Gene Pulser (Bio-Rad, Richmond, Calif.) in 0.2-cm cuvettes. Alternatively, a 0.8-ml cell suspension volume was used in a 0.4-cm cuvette with two pulses at 850 V and 25 μF (22a). The cells were then diluted with 9.5 ml of complete BHK medium (5% fetal calf serum, 10% tryptose phosphate broth in Dulbecco modified Eagle medium), plated at 37°C for 2 h, and then incubated at 37 or 28°C as indicated in the figure legends.

Preparation of [^{35}S]methionine-cysteine-labeled WT and mutant viruses. BHK cells were electroporated with WT or mutant RNA as described above, and 1×10^7 to 1.5×10^7 electroporated cells were plated in a 75-cm^2 tissue culture flask for 6 h at 37°C. The cells were then labeled at 28°C with 110 μCi of [^{35}S]methionine-cysteine (PRO-MIX; Amersham, LifeScience) per ml for 18 to 24 h. At the end of the incubation, the medium was harvested and the cell debris was removed by centrifugation at 10,000 rpm for 30 min at 4°C in a Sorvall SS34 rotor (DuPont, Newton, Conn.). The supernatant was layered over 2.5 ml of 25% (wt/wt) sucrose in 50 mM Tris (pH 7.4)–100 mM NaCl and centrifuged at 40,000 rpm for 3.5 h in an SW41 rotor at 4°C, and the virus pellet was resuspended in 300 μl of (morpholino)ethanesulfonic acid (MES)-saline buffer (20 mM MES [pH 7.0], 130 mM NaCl) and stored at −70°C.

Velocity gradient sedimentation of virus particles. Purified, radiolabeled viruses prepared as described above were layered on linear 15 to 30% (wt/vol) sucrose gradients in 200 mM NaCl–50 mM Tris (pH 7.4)–1 mM EDTA (12). Gradients were centrifuged for 60 min at 36,000 rpm at 4°C in an SW41 rotor. Fractions were collected from the bottom, and radioactivity was determined by liquid scintillation counting.

Electron microscopy of virus-infected cells. BHK cells were electroporated with WT or mutant RNA, plated on 35-mm-diameter dishes, and incubated either for 6 h at 37°C or for 2 h at 37°C and then incubated overnight at 28°C. The cells were fixed in 2.5% glutaraldehyde in 0.1 M cacodylate buffer for 40 min at room temperature, washed in 0.1 M cacodylate buffer, osmicated, dehydrated, and embedded in LX112 (Ladd Research, Burlington, Vt.). Thin sections were stained with uranyl acetate and lead citrate and examined in a 1200EX electron microscope (JEOL, Peabody, Mass.).

Analysis of protein expression pattern in electroporated cells. BHK cells electroporated with either WT-IC, G91D, or G91A RNA were plated in 35-mm-diameter dishes for 2 h at 37°C and further incubated at 37 or 28°C as indicated in the figure legends. The cells were preincubated in methionine-cysteine-deficient medium for 10 to 15 min at 37°C or for 15 to 25 min at 28°C and pulsed with 100 μCi of [^{35}S]methionine-cysteine in 0.5 ml of this medium. Cells were washed twice in Dulbecco modified Eagle medium and chased in Dulbecco modified Eagle medium containing 0.2% BSA and a 10-fold excess of unlabeled methionine-cysteine. At the end of incubation, the chase medium was removed and the cells were lysed in Triton X-100-containing lysis buffer as previously described (19) or in Nonidet P-40 (NP-40) lysis buffer (1% NP-40, 50 mM Tris [pH 7.4], 150 mM NaCl, 2 mM EDTA, 1 mg of BSA per ml, 1% aprotinin, 1 mM phenylmethylsulfonyl fluoride [PMSF], 1 μg of pepstatin per ml, 1 μg of leupeptin per ml) (40) and the nuclei were pelleted for 10 min in a microcentrifuge at maximum speed in the cold. Protease inhibitors were added to the chase medium (0.5 mM PMSF, 1 μg of pepstatin per ml, 10 μg of leupeptin per ml), and the cell debris was pelleted by centrifugation at 10,000 rpm for 20 min in a Sorvall SS34 rotor at 4°C (28). The supernatant was collected, and Triton X-100 or NP-40 was added to a 1% final concentration. Both the cell lysates and chase medium were analyzed by immunoprecipitation with a polyclonal antibody against the SFV spike protein, followed by electrophoresis on sodium dodecyl sulfate (SDS)–10% polyacrylamide gels under nonreducing conditions, all as previously described (19).

Transport of spike proteins to the cell surface. Biotinylation with sulfosuccinimidobiotin (Pierce, Rockford, Ill.), a membrane-impermeant derivatizing reagent, was used to detect the arrival of biosynthetically labeled spike proteins at the cell surface (27a, 30, 34). Electroporated cells were plated in 35-mm-diameter dishes for the indicated times at either 37 or 28°C, pulse-labeled with 50 μCi of [^{35}S]methionine-cysteine per ml, and chased as indicated. At each time point, the radiolabeled virus released in the chase medium was quantitated by immunoprecipitation as described above. The cells were placed on ice, washed twice with PBS (pH 7.4, without calcium and magnesium), and incubated for 15 min with 0.6 ml of 0.5-mg/ml sulfosuccinimidobiotin in PBS; this was followed by two identical incubations with fresh biotin. Biotin was prepared immediately before use by dilution from a stock solution (200 mg/ml of dimethyl sulfoxide). The reaction was quenched by four washes in ice-cold 10 mM Tris (pH 7.4)–150 mM NaCl–10 mM glycine. The cells were lysed in Triton X-100 lysis buffer, and the SFV spike proteins were immunoprecipitated with the rabbit polyclonal antibody as described above. Spike proteins were then released from the zysorbin by heating for 5 min at 95°C in 100 μl of 2% SDS–50 mM NaCl–10 mM Tris (pH 7.4), followed by dilution in 400 μl of NTT buffer (50 mM NaCl, 10 mM Tris [pH 7.4] containing 1% Triton X-100). The zysorbin was removed by centrifugation, and the supernatant was incubated with 50 μl of a streptavidin-agarose slurry (Pierce) for 1 h at 4°C with rotation. The streptavidin-agarose had been preblocked by rotation for 2 h at 4°C in wash buffer (1% Triton X-100, 0.2% BSA, 40 μg of PMSF per ml in PBS), followed by resuspension in NTT buffer. Following absorption of the sample, the streptavidin beads were pelleted and the supernatant was acid precipitated and resuspended in SDS sample buffer. The streptavidin beads were washed four times with wash buffer and once with PBS and resuspended in SDS sample buffer. Streptavidin beads, streptavidin supernatant, and chase medium samples were then analyzed by SDS-10% polyacrylamide gel electrophoresis (PAGE) to determine the surface, internal, and released spike proteins, respectively, at each time point.

Assays for the E1-E2 spike protein dimer. (i) Antibody coprecipitation. Radiolabeled WT-IC, G91A, and G91D viruses were solubilized on ice for 10 min in 50 mM Tris (pH 7.4 or 8.0 as indicated)–150 mM NaCl–2 mM EDTA–1% aprotinin–1 mM PMSF, 1 μg of pepstatin per ml–5 μg of leupeptin per ml containing either 1% NP-40 (40) or 1% PC-$C_{12}E_8$. The latter detergent mixture was similar to that described by Green and Claudio (11) and was composed of 1.83 mg of egg phosphatidylcholine (PC; Avanti Polar Lipids) per ml and 1% $C_{12}E_8$ (octaethylene glycol monododecyl ether; Fluka Chemical Corp., Ronkonkoma, N.Y.) in an ~1:7 molar ratio of $C_{12}E_8$ to PC. The solubilized virus samples were then immunoprecipitated with previously characterized MAbs against the E1 (MAb E1-1) or E2 (MAb E2-3) subunit (16, 19) as previously described (16, 40) but with the indicated detergent throughout. In some experiments, radiolabeled, electroporated cells were similarly lysed and analyzed by coprecipitation.

(ii) Sucrose gradient sedimentation assay. ^{35}S-labeled SFV or WT-IC, G91A, or G91D virus was incubated for 10 min at 4°C in 300 μl of a solution of MNT buffer (20 mM MES [pH 7.4], 30 mM Tris, 100 mM NaCl) containing 1%

NP-40 or PC-$C_{12}E_8$. The virus samples were analyzed by centrifugation on 5 to 12.5% (wt/wt) sucrose gradients in MNT buffer containing 0.1% NP-40 or PC-$C_{12}E_8$, 1 mM PMSF, 1% aprotinin, and 1 μg of pepstatin per ml in an SW41 rotor at 39,000 rpm for 22 h at 4°C (40).

(iii) Chymotrypsin sensitivity assay. The differential chymotrypsin sensitivity of monomeric and dimeric spike protein subunits had been suggested by previous experiments (14). It was confirmed by separation of SFV spike protein monomers and dimers by sucrose gradient sedimentation and chymotrypsin digestion of the monomer and dimer peaks (6a). The chymotrypsin sensitivity of detergent-solubilized WT-IC and mutant virus samples was determined by digestion with 0.05, 2.5, and 5.0 μg of *N*-α-*p*-tosyl-L-lysine chloromethyl ketone–chymotrypsin for 10 to 15 min on ice.

(iv) Chemical cross-linking of E1 and E2. The cross-linkers used were dimethyl-3,3′-dithiobispropionimidate · 2HCl (Pierce), a cleavable imidoester cross-linker with a 1.19-nm span, and 3,3′-dithiobis(sulfosuccinimidylpropionate) (Pierce), a water-soluble, membrane impermeable, thiol-cleavable cross-linker with a 1.2-nm span, at a final concentration of 0.25 or 5.0 mM. Purified, ^{35}S-labeled WT-IC and G91D virus preparations were diluted in 10 mM HEPES (pH 8.0–150 mM NaCl containing 1% NP-40 as indicated and incubated on ice for 10 min. Aliquots (100 μl) of the samples were then mixed with 100 μl of freshly prepared cross-linker solutions in 200 mM triethanolamine (pH 8.2) and incubated for 60 min at room temperature. The reaction was terminated and concentrated by acid precipitation, and the samples were solubilized by addition of SDS sample buffer and incubation at 95°C [3,3′-dithiobis(sulfosuccinimidyl-propionate)] or 65°C (dimethyl-3,3′-dithiobispropionimidate · 2HCl). The samples and molecular weight markers (Sigma Chemical Co., St. Louis, Mo.) were analyzed by electrophoresis on SDS–5 to 10% gradient polyacrylamide gels.

RESULTS

Effects of temperature on assembly of WT and mutant viruses. Our previous analysis of mutations in the putative fusion peptide was based on transient expression of the spike protein in COS cells (22). To analyze the effects of the G91A and G91D mutations in virus, *Cla*I restriction fragments containing the WT or mutant sequences were subcloned into the pSP6-SFV4 infectious SFV clone (23) and transcribed in vitro to give infectious RNA. BHK cells were infected with WT-IC or mutant RNAs by electroporation at high efficiency (23). Expression of spike proteins and their assembly and release from the cells at 37°C were then evaluated by pulse-chase analysis and immunoprecipitation (Fig. 1A). As expected from our previous studies, cells expressing any of the three constructs produced abundant p62 and E1 and cleaved the p62 precursor to E2 and E3 during the 90-min chase period (E3 is not resolved on this gel system). Analysis of the chase medium showed that cells infected with the WT-IC construct released intact E1 and E2. In contrast, the chase medium from either G91A or G91D at 37°C showed little or no protein migrating at the positions of authentic E1 and E2; instead, a prominent radiolabeled protein migrating slightly below the position of native E1 was released. Sedimentation analysis of the chase medium demonstrated that WT-IC spike proteins were released in assembled virions and that little mutant spike protein was assembled into virus (data not shown). Precipitation with subunit-specific MAbs showed that the spike protein released from mutant infected cells was predominantly a soluble truncated form of E1 and that little E2 was released into the medium (data not shown). Variable amounts of cleaved E1 were also released from WT-IC-infected cells but constituted a much smaller proportion of the total E1 released. Thus, the G91D and G91A mutations appeared to inhibit virus assembly at 37°C and resulted in production of a truncated form of the E1 subunit. This cleavage was unaffected by the inclusion of pepstatin, leupeptin, aprotinin, and PMSF in the chase medium (data not shown).

Release of truncated E1 was previously observed when the SFV spike proteins were expressed in the infectious clone in the absence of nucleocapsid, conditions under which budding cannot take place (43). Since all of the virus structural components were expressed in our system, it was possible that the

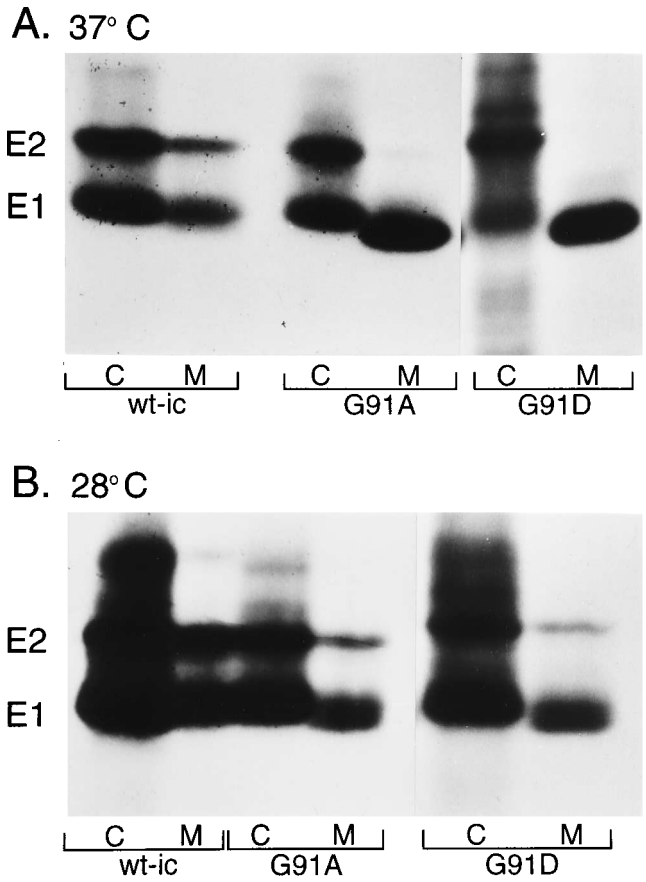

FIG. 1. Assembly phenotype of G91A, G91D, and WT-IC SFVs at 37 and 28°C. BHK cells were electroporated with WT-IC, G91A, or G91D RNA and cultured at 37 or 28°C, and virus protein expression was evaluated by pulse-chase analysis with [^{35}S]methionine-cysteine. The labeled virus spike proteins in the cells and medium were analyzed by immunoprecipitation and SDS–10% PAGE. (A) Cells were incubated for 6 h at 37°C to permit virus expression and then pulsed for 15 min and chased for 90 min at 37°C. (B) Cells were incubated for 2 h at 37°C and then overnight at 28°C; this was followed by a 60-min pulse and a 7-h chase at 28°C.

G91A and G91D mutations instead affected the efficiency of virus protein interactions and thereby prevented budding. We reasoned that the efficiency of viral protein-protein interactions might be improved by incubation of infected cells under conditions potentially less stringent for such interactions, such as reduced temperature. Infected cells were therefore incubated overnight at 28°C, and the assembly and release of virus spike proteins were then assayed at this reduced temperature (Fig. 1B). Under these conditions, both E2 and E1 were released intact from cells infected with either G91A or G91D. The proportion of intact E1 released was somewhat variable and was estimated visually to be 30 to 50% of the total E1 released in this and similar experiments. This result suggested that virus assembly occurred and that proteolysis of E1 to the truncated form was inhibited. Production of the small amounts of truncated E1 from WT-IC-infected cells was also reduced. Qualitatively similar results were obtained by using 1 to 20-h chase periods. These data indicated that the assembly phenotype of the G91A and G91D mutants was strongly temperature sensitive.

The thermoreversibility of the mutant assembly phenotype was examined for G91D by using pulse-chase analysis performed at combinations of the restrictive (37°C) and permis-

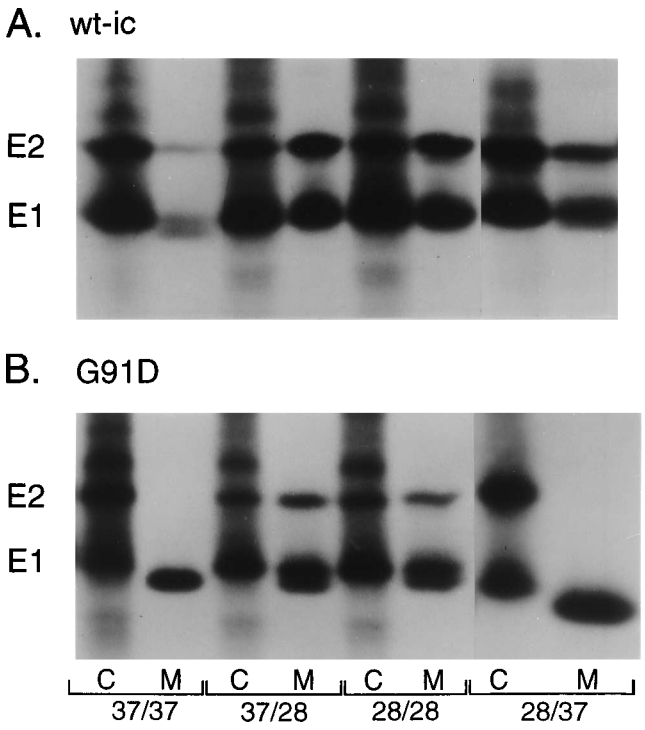

FIG. 2. Reversibility of temperature effects on G91D assembly. BHK cells were electroporated with WT-IC (A) or G91D (B) RNA and plated for 2 h at 37°C; this was followed by further incubation for either 4 h at 37°C (first six lanes of each panel) or 22 h at 28°C (last two lanes of each panel). Virus spike protein expression and assembly were then analyzed by pulse-chase labeling, immunoprecipitation, and SDS–10% PAGE. The pulse-chase analyses were performed at the temperatures indicated as follows: the first number is the pulse temperature and the second number is the chase temperature in degrees Celsius. We used 20-min pulse and 90 to 120-min chase times for 37°C samples and 60-min pulse and overnight chase times for 28°C samples.

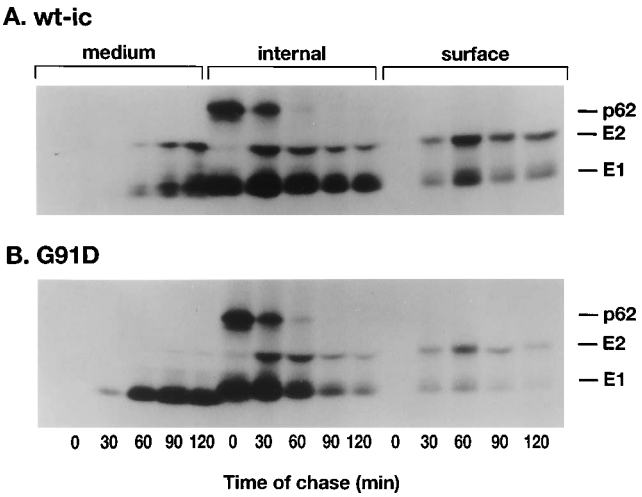

FIG. 3. Transport of WT and G91D spike proteins to the cell surface at 37°C. BHK cells were electroporated with WT-IC (A) or G91D (B) RNA and plated for 6 h at 37°C. Cells were then pulse-labeled for 15 min and chased for the times indicated, all at 37°C. At each time point, the medium was harvested and saved for immunoprecipitation analysis and the cells were placed on ice and derivatized with sulfosuccinimidobiotin. The cells were then lysed, and the virus spike proteins were precipitated and separated into surface and internal proteins by streptavidin binding. The samples were analyzed by SDS–10% PAGE.

sive (28°C) temperatures. BHK cells were electroporated with WT-IC or G91D RNA, plated at 37°C for 6 h, and radiolabeled (first six lanes of Fig. 2A and B). As previously observed in Fig. 1, G91D-infected cells pulsed and chased at 37°C released mainly truncated E1 (37/37 lanes) while cells pulsed and chased at 28°C released intact E2 and both the intact and truncated forms of E1 (28/28 lanes). When G91D-infected cells were pulsed at 37°C and chased at 28°C, (37/28 lanes), intact E1 and E2 were released, demonstrating that protein synthesized during a pulse at the nonpermissive temperature could be assembled into virus during a chase at the permissive temperature. As shown below (see Fig. 5 and 6), the intact released spike proteins were assembled into virus particles similar to WT SFV.

BHK cells were also electroporated with WT-IC and G91D RNAs and plated overnight at the permissive temperature (last two lanes of Fig. 2A and B). The cells were then pulsed for 60 min at 28°C and chased for 2 h at 37°C. Even though the G91D-infected cells were incubated and pulse-labeled at 28°C, a shift to the restrictive temperature during the chase period resulted in release of the truncated form of E1 (28/37 lanes of Fig. 2B). Little intact E1 or E2 was released into the medium. Similar results were obtained with the G91A mutant (data not shown). In contrast, WT-IC-expressing cells (Fig. 2A) released intact E2 and E1 following incubation at any combination of 37 and/or 28°C.

Taken together, these data indicate that incorporation of mutant spike glycoproteins into virions was dependent on the incubation temperature during virus assembly and budding but not during spike protein biosynthesis. In addition, the temperature-sensitive assembly phenotype of the mutants was found to be maintained following 22 h of incubation at 28°C (last two lanes of Fig. 2B). Thus, appreciable reversion of the mutants to the WT phenotype did not occur during this time period at 28°C.

Transport of mutant spike proteins to the cell surface and association with virus nucleocapsids. Since little G91D or G91A virus was assembled at the restrictive temperature, transport of the mutant spike proteins to the site of budding, the cell plasma membrane, was examined at 37°C. WT-IC- or G91D-infected cells were pulse-labeled for 15 min and chased for various times, all at the nonpermissive temperature. At each time point, the arrival of newly synthesized spike proteins at the plasma membrane was detected by cell surface labeling with biotin, and the internal, nonbiotinylated virus spike proteins and labeled virus released into the chase medium were also immunoprecipitated and evaluated by SDS-PAGE (Fig. 3). The pattern of internal proteins showed that the kinetics of p62 cleavage were similar for WT-IC and G91D. Starting with a 30-min chase, E1 and E2 spike protein subunits from both the WT and the mutant were detected at the plasma membrane by biotin labeling. These data are in keeping with our previous immunofluorescence and radioimmunoassay data on the expressed mutant spike protein, which indicated that both spike protein subunits were transported to the plasma membrane (22). Notably, however, the proportion of mutant E1 and E2 that was derivatized with biotin was less than that of the WT-IC. This appeared to be due to rapid release of truncated E1 into the medium at 37°C, starting with a 30-min chase, and the presumed degradation of E2. In contrast, release of WT-IC spike proteins was not observed until the 60-min chase period. A similar analysis at 28°C indicated that the cell surface transport rates of G91D and WT-IC spike proteins were also comparable at this temperature (data not shown). Under 28°C conditions, at which mutant spike protein cleavage was inhibited, the proportion of G91D spike proteins at the cell surface was more similar to that of WT-IC (data not shown).

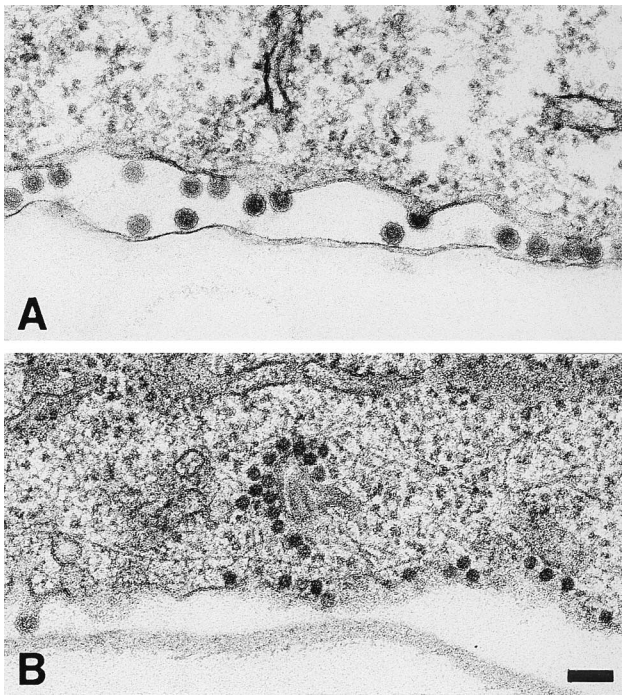

FIG. 4. Electron microscopy of WT and G91D virus-infected cells incubated at 37°C. BHK cells were electroporated with WT-IC (A) or G91D (B) RNA, incubated at 37°C for 6 h, and processed for electron microscopy. The area shown is the basal domain of each cell, and the line beneath each cell represents the dish surface. Bar, 0.1 μm.

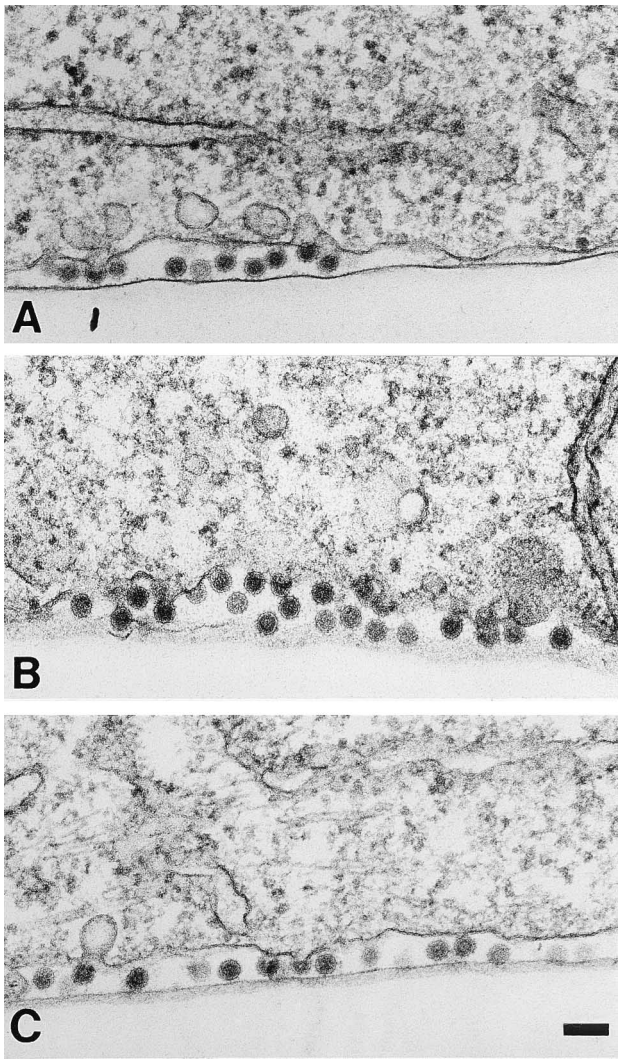

FIG. 5. Electron microscopy of WT and mutant virus-infected cells incubated at 28°C. BHK cells were electroporated with viral RNAs and incubated at 37°C for 2 h; this was followed by overnight incubation at 28°C and processing for electron microscopy. The basal domain of each cell is shown. Panels: A, WT-IC; B, G91A; C, G91D. Bar, 0.1 μm.

Since the G91D mutant spike proteins were transported to the plasma membrane but not released in mature virus particles, electron microscopy was used to determine if the mutant spike proteins were associated with viral nucleocapsids. BHK cells were electroporated with WT-IC or G91D RNA, incubated at 37°C for 6 h, and fixed and processed for electron microscopy (Fig. 4A). The morphology of cells infected with WT-IC revealed numerous typical SFV particles and budding virions, particularly at the basolateral domain of the cells. It is known that SFV budding is targeted to the basolateral domain of polarized epithelial cells (33), although BHK cells infected under normal culture conditions do not show strongly polarized budding of SFV. In contrast to cells infected with the WT, cells infected with the G91D mutant at 37°C showed accumulation of electron-dense nucleocapsids beneath the plasma membrane, as well as nucleocapsids associated with intracellular membranes (Fig. 4B). Occasional single-core virus particles or forming virions were also observed (left side of Fig. 4B). Similar results were obtained with the G91A mutant at 37°C, although somewhat more assembled virus particles were observed (data not shown). These observations confirm the impaired release of mutant virus particles observed in the pulse-chase studies. It is known that SFV nucleocapsid association with the plasma membrane requires the presence of plasma membrane spike proteins containing a functional E2 cytoplasmic domain (44). Our data therefore suggest that at 37°C the mutant spike proteins were transported to the plasma membrane, where the E2 cytoplasmic domain interacted with the virus nucleocapsid, but that subsequent virus assembly and budding were inhibited.

Characterization of mutant virus produced at 28°C. In contrast to the results obtained at 37°C, the pulse-chase data suggested that mutant virions were assembled during incubation of infected cells at 28°C. To evaluate the morphology of virion production at this temperature, BHK cells were electroporated with WT-IC, G91A, and G91D RNAs; incubated overnight at 28°C; and fixed and processed for electron microscopy. Abundant released virus particles and budding virions were observed in all three samples at this temperature (Fig. 5). The virions contained a single electron-dense nucleocapsid and appeared to be similar in overall structure and diameter.

To further characterize the structure of mutant virions assembled at 28°C, virus was radiolabeled with [^{35}S]methionine-cysteine during growth at the permissive temperature and purified by pelleting through a sucrose cushion. The labeled virions were then analyzed by velocity sedimentation on 15 to 30% sucrose gradients, a technique successfully used to detect multicore virus particles in the *ts*103 mutant of Sindbis virus (12). WT-IC, G91A, and G91D virus preparations showed a single major peak of radioactivity sedimenting from fractions 22 to 26 (Fig. 6). Thus, G91D and G91A virions assembled at 28°C appeared to be morphologically and physically similar to WT-IC virions.

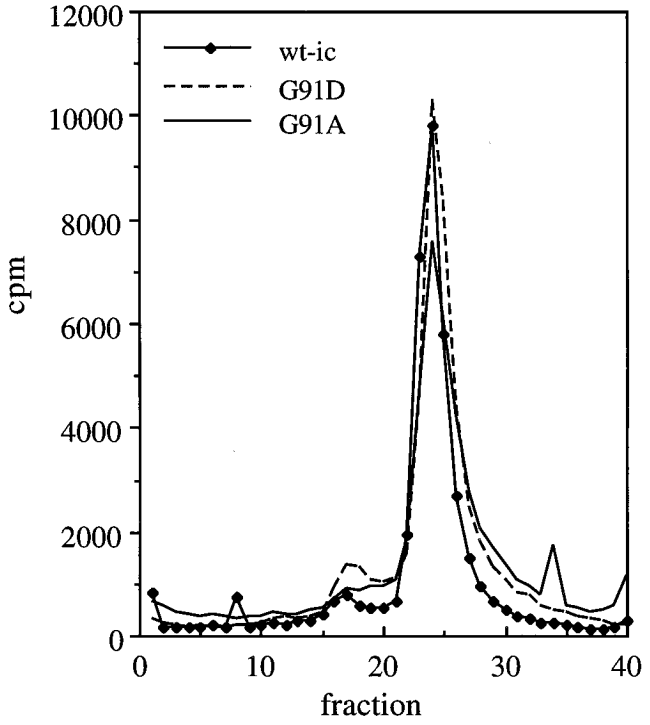

FIG. 6. Velocity gradient sedimentation analysis of mutant and WT virions. Purified, ^{35}S-labeled preparations of WT-IC, G91A, and G91D SFVs grown at 28°C were analyzed by sedimentation on 15 to 30% (wt/vol) sucrose gradients (in buffer without detergent). Centrifugation was for 60 min at 36,000 rpm in an SW41 rotor at 4°C. The bottom of each gradient is fraction 1.

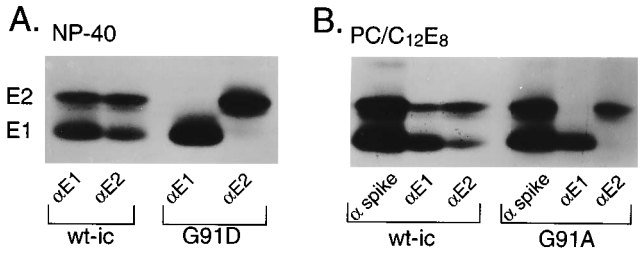

FIG. 7. Coimmunoprecipitation analysis of WT and mutant virus spike proteins. Purified, ^{35}S-labeled preparations of WT-IC, G91A, and G91D SFVs grown at 28°C were solubilized with either 1% NP-40 in buffer at pH 8.0 (A) or a 1% PC-$C_{12}E_8$ detergent mixture in buffer at pH 7.4 (B) (see Materials and Methods). Samples were immunoprecipitated with either a rabbit polyclonal anti-spike antibody (αspike) or MAb E1-1 (αE1) or E2-3 (αE2) and analyzed by SDS–10% PAGE.

Effects of the G91D and G91A mutations on spike protein dimerization. The temperature sensitivity of G91D and G91A assembly suggested a potential defect in virus protein interactions. Since at 37°C mutant spike proteins were transported to the plasma membrane and associated with nucleocapsids, we reasoned that the block in budding might be in later stages of virus assembly that require lateral spike protein interactions (7). An effect of the mutations on such lateral spike protein interactions could be due to an altered conformation of the E1-E2-E3 protomer that oligomerizes to form the spike protein trimer. We therefore examined the dimeric interaction between the E1 and p62/E2 spike protein subunits by using WT-IC and mutant virions radiolabeled and assembled at 28°C.

E1-E2 subunit association was first assayed by coimmunoprecipitation of ^{35}S-labeled virus with E1- or E2-specific MAbs (19) under conditions of detergent lysis that preserve the dimer (16, 40). The WT-IC E1 and E2 subunits were efficiently coprecipitated in an NP-40 lysis buffer (Fig. 7A), while the spike protein subunits from the G91D mutant (Fig. 7A) or the G91A mutant (data not shown) did not coprecipitate under these conditions. Coprecipitation analysis was then performed in PC-$C_{12}E_8$. This detergent mixture has a lower chemical potential than NP-40, and a similar mixture of PC and the analogous detergent Lubrol PX was found to preserve assembly intermediates of the acetylcholine receptor (11). As shown in Fig. 7B, the WT-IC E1-E2 spike protein dimer was efficiently coprecipitated in PC-$C_{12}E_8$ while E1 and E2 from G91A (Fig. 7B) and G91D (data not shown) did not coprecipitate. BHK cells infected with WT-IC, G91D, or G91A at either 37 or 28°C were pulse-labeled, lysed with NP-40 buffer, and similarly assayed by coprecipitation (data not shown). In keeping with previous results (16, 40), WT-IC E1 was detected predominantly in a dimeric interaction with the p62 precursor protein and the mature E2 subunit. In contrast, no evidence of a mutant E1 dimer with either p62 or E2 was observed in cells infected and labeled at either temperature.

These results suggested that the spike protein dimer was either not present in the mutants, not stable to detergent lysis, or dissociated by binding of the MAbs. Since it is known that antibody binding can cause dissociation of the spike dimer (45), sucrose gradient centrifugation of NP-40-treated virus was used to assay for the E1-E2 dimer in the absence of antibody interactions. As shown in Fig. 8, the WT-IC virus spike protein sedimented as a dimer peak centered at fraction 29 and a smaller monomer peak centered at fraction 35. In contrast, G91D spike proteins sedimented exclusively as mono-

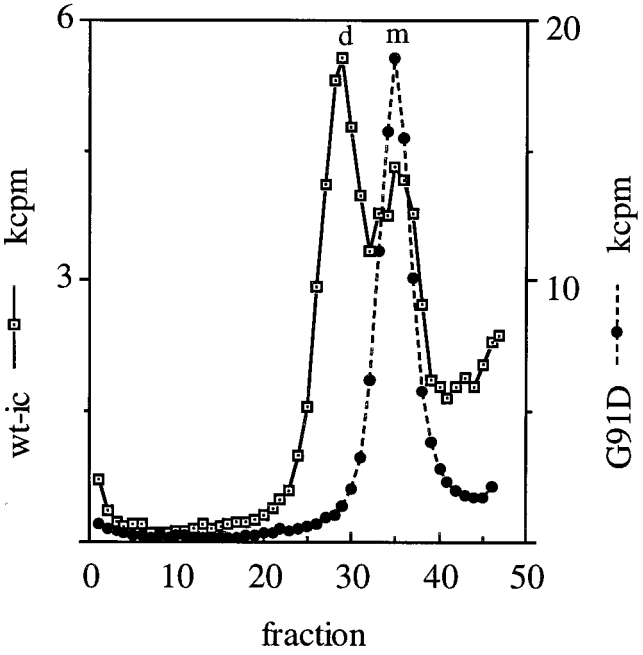

FIG. 8. Gradient sedimentation analysis of WT and G91D spike proteins. Purified, ^{35}S-labeled preparations of WT-IC and G91D SFVs grown at 28°C were solubilized with 1% NP-40 and analyzed by centrifugation on a 5 to 12.5% (wt/wt) sucrose gradient (in buffer containing 0.1% NP-40). The gradient was centrifuged for 22 h at 4°C in an SW41 rotor at 39,000 rpm and fractionated, and the radioactivity was determined. The bottom of the gradient is fraction 1. The positions of the spike protein monomer (m) and dimer (d) peaks are indicated.

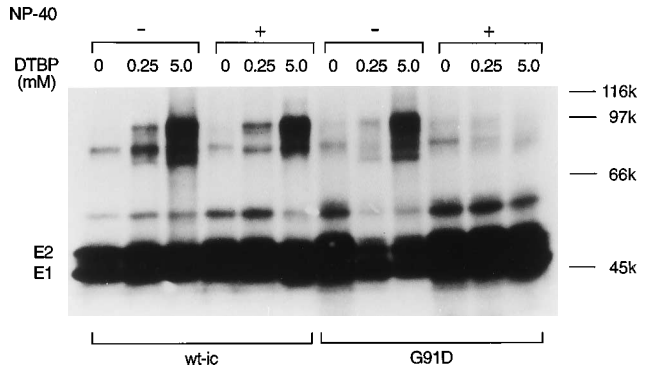

FIG. 9. Chemical cross-linking of spike proteins from WT and G91D SFVs in the presence and absence of detergent. Purified, ^{35}S-labeled preparations of WT-IC and G91D SFVs grown at 28°C were diluted in ice-cold buffer with or without 1% NP-40 as indicated at the top. The samples were then treated with the concentrations of the chemical cross-linker dimethyl-3,3′-dithiobispropionimidate · 2HCl (DTBP) as indicated above the lanes for 60 min at room temperature. Samples were precipitated with trichloroacetic acid, dissolved in SDS sample buffer at 65°C, and analyzed by SDS–5 to 10% PAGE. The positions of the molecular mass markers (45, 66, 97, and 116 kDa) are shown on the right.

mers. Further gradient analysis with the PC-$C_{12}E_8$ detergent mixture or the G91A mutant virus gave similar results (data not shown).

Oligomerization of newly synthesized virus spike proteins frequently results in conversion to protease resistance (6). Our previously published pulse-chase data suggested that the SFV spike heterodimer was resistant to chymotrypsin cleavage, while newly synthesized monomeric E1 and E2 were chymotrypsin sensitive (14). This differential protease sensitivity was confirmed by chymotrypsin digestion of gradient-separated dimers and monomers of WT E1 and E2 (data not shown). The protease sensitivities of the WT-IC, G91A, and G91D viruses were then characterized following solubilization in an NP-40-containing buffer at pH 7.4. WT spike subunits were relatively resistant to chymotrypsin, while both the G91A and G91D mutant spike subunits were chymotrypsin sensitive (data not shown).

Thus, under three different assay conditions that preserve the WT-IC heterodimer, the G91D and G91A spike proteins were monomeric. However, the E1 and E2 spike protein subunits from either mutant were both transported efficiently to the plasma membrane (Fig. 3 and reference 22) and were assembled into icosahedral virus particles at 28°C (Fig. 5 and 6). Studies of WT spike protein biosynthesis indicate that the E1 and E2 subunits dimerize in the rough endoplasmic reticulum and suggest that E1 must be oligomerized with p62 to be transported to the plasma membrane (4, 21, 31, 46). The mutant spike protein transport data thus suggested that the spike protein was dimeric at either 37 or 28°C. Notably, all three of the dimer assays described above depended on detergent solubilization. We therefore assayed for E1-E2 dimers by chemical cross-linking of radiolabeled WT-IC and mutant virus particles in the presence or absence of the detergent NP-40. The cross-linked spike protein dimer should migrate at ~100 kDa on SDS-PAGE. As shown in Fig. 9, the WT-IC spike protein dimer was efficiently cross-linked with dimethyl-3,3′-dithiobispropionimidate · 2 HCl to yield a band in the approximate position of the 97-kDa molecular mass marker. In agreement with previous studies (18, 45), cross-linking of the WT-IC dimer was unaffected by the presence or absence of NP-40. In the absence of detergent, the G91D mutant spike protein was similarly cross-linked and produced the ~100-kDa dimer band with an efficiency comparable to that of WT-IC. In contrast, however, in the presence of NP-40 the mutant spike heterodimer was not cross-linked. Similar cross-linking patterns resulted when another cross-linker, 3,3′-dithiobis(sulfosuccinimidylpropionate), was used (data not shown). Thus, the G91D mutant spike proteins appear to assemble into virions as an E1-E2 dimer, but this dimer is less stable than that of the WT virus.

DISCUSSION

Alphaviruses have an icosahedral symmetry in both their nucleocapsids and their spike protein shells (reviewed in references 17 and 37). These two virus components are separated by the virus lipid bilayer membrane and connected by the transmembrane domain and internal tail of the E2 subunit. The icosahedral nucleocapsid can be formed in the absence of spike proteins (38), and the spike proteins are transported to the plasma membrane in the absence of nucleocapsid (43), but the very ordered and interdependent organization of the spike proteins and nucleocapsid is reflected in the fact that both are required for the budding of alphavirus particles (38). We have here characterized two temperature-sensitive SFV mutants, G91A and G91D, which assemble morphologically normal virus particles at 28°C but little or no virus at 37°C. At the nonpermissive temperature, the mutations block budding at a step after spike protomer transport to the plasma membrane and nucleocapsid binding and cause the release of a truncated fragment of E1 into the medium.

Our E1 mutants show some similarities to other alphavirus mutants that have been previously described. When SFV spike proteins are expressed in the absence of nucleocapsid, both the E1 and E2 subunits are localized to the plasma membrane but no budding occurs and a truncated E1 fragment is released into the medium (43). The interaction of the spike protein with the nucleocapsid is mediated by the 31-amino-acid internal domain of E2. Residues across the entire E2 tail appear to be important for efficient nucleocapsid binding, and the active form for binding may be an oligomer of the E2 tail (reviewed in references 17 and 37). Mutation of a highly conserved tyrosine residue within the N-terminal half of the tail produces budding-incompetent spike proteins (44). Both the E1 and E2 subunits from such mutant spikes are correctly transported to the plasma membrane but are unable to bind nucleocapsids. Several of these mutations also cause the production of various amounts of truncated E1 (7, 44).

Lateral interactions between the spike proteins take place as part of the protomer trimerization [$(E1\text{-}E2\text{-}E3)_3$] and further oligomerization that are involved in spike lattice formation and budding. Such lateral interactions can be directly demonstrated by the cross-linking of virus particles or of spike proteins at the cell surface (1, 32) or by the rescue of budding-incompetent spike protomers through their association with budding-competent spike protomers (7). Fluorescence photobleaching techniques reveal that spike proteins are mobile within the plane of the bilayer at early times of infection but become immobilized at later times (15). This probably reflects both the interaction of the spike protein with the nucleocapsid and lateral spike-spike protein associations during budding. The *ts*20 mutant of Sindbis virus contains a mutation, H291L, in the ectodomain of E2 (24). At the nonpermissive temperature, *ts*20 spike proteins are transported to the plasma membrane and associate with nucleocapsids but budding is impaired (36). Interestingly, fluorescence photobleaching studies of *ts*20 demonstrated that *ts*20 spike proteins do not become immobilized during infection, even though capsid binding oc-

curs (15). This suggests that lateral interactions between *ts*20 spike proteins are disrupted by the mutation in E2. Unlike our results obtained with the E1 mutants, *ts*20 spike proteins synthesized at the nonpermissive temperature do not appear to be significantly incorporated into virus particles at the permissive temperature (36). It is not known if a truncated fragment of E1 is released during growth of *ts*20 at the nonpermissive temperature.

Several other events may be involved in the final stages of assembly of cell surface spike proteins into virus and release of virus into the extracellular medium. The small, hydrophobic 6K polypeptide appears to be involved in virus budding from the plasma membrane (8, 23, 35). When 6K is deleted, both subunits of the spike protein reach the cell surface but virus production is impaired (23). Budding of SFV from cells is also inhibited in the absence of cellular cholesterol (28). Cholesterol depletion does not affect spike protein localization to the plasma membrane or cause production of a truncated fragment of E1 (28). Experiments with protein kinase and phosphatase inhibitors have, in addition, suggested a role for phosphorylation and dephosphorylation in virus production (25).

On the basis of this knowledge of the alphavirus exit pathway, several possible explanations for the budding phenotype of the G91A and G91D mutants are suggested. One hypothesis is that the mutations in the E1 subunit could act indirectly to produce an altered conformation of the E2 cytoplasmic tail that inefficiently and nonproductively recognizes its binding site in the capsid protein. Another possibility is that the mutant form of the spike protomer is inherently more susceptible to proteolytic cleavage, which reduces the plasma membrane concentration of otherwise budding-competent spikes. Alternatively, the mutant spike protomers could bind nucleocapsid correctly but be unable to form the spike trimer and/or assume the proper T=4 icosahedral spacing required for budding. In this model, proteolysis of mutant spike subunits would be a consequence of their lack of assembly into virus rather than its cause.

Although the data reported here do not permit us to definitively identify the mechanism of the budding defect, we favor a model involving impaired lateral spike protein interactions in the mutants. The electron microscopy results (Fig. 4) argue that the E2 cytoplasmic domain in the mutants does bind nucleocapsid with reasonable efficiency, since abundant membrane-localized nucleocapsids were observed. It is also clear that cleavage of E1 can occur with the WT spike protein, although to a lesser extent than with the mutant. In addition, a soluble E1 fragment with a comparable molecular weight is generated by in vitro proteinase K digestion of virus in nonionic detergent (18, 20). The similarity of in vivo cleavage and in vitro cleavage implies that the E1 subunit has a protease-susceptible "hinge" region that is made accessible to cleavage when the normal icosahedral spike shell is disrupted by detergent treatment or an assembly defect.

The effects of the mutations on virus assembly suggest that the sequence of the fusion peptide has evolved to permit both optimal virus fusion and the most efficient folding and interaction between the E1 and E2 subunits. Similar to the structure of the influenza virus fusion protein (3, 42), the hydrophobic fusion peptide of SFV may be shielded from water by its assembly into the interior of the spike protein. Even the seemingly minor substitution of alanine for glycine could disrupt the packing between the subunits, resulting in the observed decrease in E1-E2 dimer stability and an inhibition of further spike protomer oligomerization required for budding. Retention of the mutant spike protomer at the plasma membrane for unusually long periods in the absence of the normal protective lateral interactions might then result in its increased cleavage. If the spike protomer does not trimerize, this could also have secondary effects on the binding of the E2 tail to the nucleocapsid, further reducing the possibility of budding.

In conclusion, we have characterized the effects of the G91D and G91A mutations on the assembly and spike protein interactions of SFV. Both mutations produced a strong block in virus assembly that was partially reversed by growth at reduced temperature. This effect of the mutations correlated with decreased stability of the E1-E2 dimer, suggesting that the mutations reduced the efficiency of the lateral spike protein interactions required for virus budding. Virus particles containing the mutations can be produced by growth at the permissive temperature. Our previous studies of the effects of the mutations on cell-cell fusion suggest that the mutant virus particles would have defects in infectivity and membrane fusion. Indeed, the G91D and G91A viruses have impaired infectivity at either 28 or 37°C (17a). Such mutant virions are now being characterized to determine the step in the fusion pathway that is affected.

ACKNOWLEDGMENTS

We thank Frank Macaluso and the members of the Analytical Ultrastructure Center of Albert Einstein for assistance with electron microscopy and Susan Jeffrey for help with the infectious clone and electroporation. We thank Peter Liljeström and Henrik Garoff for SFV infectious clone pSP6-SFV4 and helpful suggestions on its use. Carolyn Machamer and Marianne Marquardt provided useful advice on the biotinylation experiments. We also thank the members of our laboratory for their input and Duncan Wilson and Dennis Shields for critical reading of the manuscript.

This work was supported by grants to M. Kielian from the American Cancer Society (VM-41), the Hirschl Charitable Trust, and the Pew Scholars Program in the Biomedical Sciences and by Cancer Center Core Support grant NIH/NCI P30-CA13330. W. Duffus was supported by NIH F31 GM12301, and P. Levy-Mintz was supported by NIH training grant T32 CA09060.

REFERENCES

1. **Anthony, R. P., and D. T. Brown.** 1991. Protein-protein interactions in an alphavirus membrane. J. Virol. **65:**1187–1194.
2. **Bentz, J.** 1993. Viral fusion mechanisms, p. 1–529. CRC Press, Inc., Boca Raton, Fla.
3. **Bullough, P. A., F. M. Hughson, J. J. Skehel, and D. C. Wiley.** 1994. Structure of influenza haemagglutinin at the pH of membrane fusion. Nature (London) **371:**37–43.
4. **Cutler, D. F., and H. Garoff.** 1986. Mutants of the membrane-binding region of Semliki Forest virus E2 protein. I. Cell surface transport and fusogenic activity. J. Cell Biol. **102:**889–901.
5. **deCurtis, I., and K. Simons.** 1988. Dissection of Semliki Forest virus glycoprotein delivery from the trans-Golgi network to the cell surface in permeabilized BHK cells. Proc. Natl. Acad. Sci. USA **85:**8052–8056.
6. **Doms, R. W., R. A. Lamb, J. K. Rose, and A. Helenius.** 1993. Folding and assembly of viral membrane proteins. Virology **193:**545–562.

6a. **Duffus, W. A.** Unpublished data.

7. **Ekström, M., P. Liljeström, and H. Garoff.** 1994. Membrane protein lateral interactions control Semliki Forest virus budding. EMBO J. **13:**1058–1064.
8. **Gaedigk-Nitschko, K., M. Ding, M. A. Levy, and M. J. Schlesinger.** 1990. Site-directed mutations in the Sindbis virus 6K protein reveal sites for fatty acylation and the underacylated protein affects virus release and virion structure. Virology **175:**282–291.
9. **Garoff, H., A.-M. Frischauf, K. Simons, H. Lehrach, and H. Delius.** 1980. Nucleotide sequence of cDNA coding for Semliki Forest virus membrane glycoproteins. Nature (London) **288:**236–241.
10. **Garoff, H., J. Wilschut, P. Liljeström, J. M. Wahlberg, R. Bron, M. Suomalainen, J. Smyth, A. Salminen, B. U. Barth, and H. Zhao.** 1994. Assembly and entry mechanisms of Semliki Forest virus. Arch. Virol. **9:**329–338.
11. **Green, W. N., and T. Claudio.** 1993. Acetylcholine receptor assembly: subunit folding and oligomerization occur sequentially. Cell **74:**57–69.
12. **Hahn, C. S., C. M. Rice, E. G. Strauss, E. M. Lenches, and J. H. Strauss.** 1989. Sindbis virus *ts*103 has a mutation in glycoprotein E2 that leads to defective assembly of virions. J. Virol. **63:**3459–3465.
13. **Helenius, A., J. Kartenbeck, K. Simons, and E. Fries.** 1980. On the entry of

Semliki Forest virus into BHK-21 cells. J. Cell Biol. **84:**404–420.
14. **Jain, S. K., S. DeCandido, and M. Kielian.** 1991. Processing of the p62 envelope precursor protein of Semliki Forest virus. J. Biol. Chem. **266:**5756–5761.
15. **Johnson, D. C., M. J. Schlesinger, and E. L. Elson.** 1981. Fluorescence photobleaching recovery measurements reveal differences in envelopment of Sindbis and vesicular stomatitis viruses. Cell **23:**423–431.
16. **Justman, J., M. R. Klimjack, and M. Kielian.** 1993. Role of spike protein conformational changes in fusion of Semliki Forest virus. J. Virol. **67:**7597–7607.
17. **Kielian, M.** 1995. Membrane fusion and the alphavirus life cycle. Adv. Virus Res. **45:**113–151.
17a. **Kielian, M., W. A. Duffus, and M. R. Klimjack.** Unpublished data.
18. **Kielian, M., and A. Helenius.** 1985. pH-induced alterations in the fusogenic spike protein of Semliki Forest virus. J. Cell Biol. **101:**2284–2291.
19. **Kielian, M., S. Jungerwirth, K. U. Sayad, and S. DeCandido.** 1990. Biosynthesis, maturation, and acid activation of the Semliki Forest virus fusion protein. J. Virol. **64:**4614–4624.
20. **Klimjack, M. R., S. Jeffrey, and M. Kielian.** 1994. Membrane and protein interactions of a soluble form of the Semliki Forest virus fusion protein. J. Virol. **68:**6940–6946.
21. **Kondor-Koch, C., B. Burke, and H. Garoff.** 1983. Expression of Semliki Forest virus proteins from cloned cDNA. I. The fusion activity of the spike glycoprotein. J. Cell Biol. **97:**644–651.
22. **Levy-Mintz, P., and M. Kielian.** 1991. Mutagenesis of the putative fusion domain of the Semliki Forest virus spike protein. J. Virol. **65:**4292–4300.
22a. **Liljeström, P.** Personal communication.
23. **Liljeström, P., S. Lusa, D. Huylebroeck, and H. Garoff.** 1991. In vitro mutagenesis of a full-length cDNA clone of Semliki Forest virus: the small 6,000-molecular-weight membrane protein modulates virus release. J. Virol. **65:**4107–4113.
24. **Lindqvist, B. H., J. DiSalvo, C. M. Rice, J. H. Strauss, and E. G. Strauss.** 1986. Sindbis virus mutant ts20 of complementation group E contains a lesion in glycoprotein E2. Virology **151:**10–20.
25. **Liu, N., and D. T. Brown.** 1993. Phosphorylation and dephosphorylation events play critical roles in Sindbis virus maturation. Virology **196:**703–711.
26. **Lobigs, M., Z. Hongxing, and H. Garoff.** 1990. Function of Semliki Forest virus E3 peptide in virus assembly: replacement of E3 with an artifical signal peptide abolishes spike heterodimerization and surface expression of E1. J. Virol. **64:**4346–4355.
27. **Lopez, S., J.-S. Yao, R. J. Kuhn, E. G. Strauss, and J. H. Strauss.** 1994. Nucleocapsid-glycoprotein interactions required for assembly of alphaviruses. J. Virol. **68:**1316–1323.
27a. **Machamer, C.** Personal communication.
28. **Marquardt, M. T., T. Phalen, and M. Kielian.** 1993. Cholesterol is required in the exit pathway of Semliki Forest virus. J. Cell Biol. **123:**57–65.
29. **Marsh, M., and A. Helenius.** 1989. Virus entry into animal cells. Adv. Virus Res. **36:**107–151.
30. **Matter, K., M. Brauchbar, K. Bucher, and H.-P. Hauri.** 1990. Sorting of endogenous plasma membrane proteins occurs from two sites in cultured human intestinal epithelial cells (Caco-2). Cell **60:**429–437.
31. **Melancon, P., and H. Garoff.** 1986. Reinitiation of translocation in the Semliki Forest virus structural polyprotein: identification of the signal for the E1 glycoprotein. EMBO J. **5:**1551–1560.
32. **Rice, C. M., and J. H. Strauss.** 1982. Association of Sindbis virion glycoproteins and their precursors. J. Mol. Biol. **154:**325–348.
33. **Roman, L., and H. Garoff.** 1986. Alteration of the cytoplasmic domain of the membrane-spanning glycoprotein p62 of Semliki Forest virus does not affect its polar distribution in established lines of Madin-Darby canine kidney cells. J. Cell Biol. **103:**2607–2618.
34. **Rosenwald, A., C. Machamer, and R. Pagano.** 1992. Effects of a sphingolipid synthesis inhibitor on membrane transport through the secretory pathway. Biochemistry **31:**3581–3590.
35. **Schlesinger, M. J., S. D. London, and C. Ryan.** 1993. An in-frame insertion into the Sindbis virus 6K gene leads to defective proteolytic processing of the virus glycoproteins, a *trans*-dominant negative inhibition of normal virus formation, and interference in virus shut off of host-cell protein synthesis. Virology **193:**424–432.
36. **Smith, J. F., and D. T. Brown.** 1977. Envelopment of Sindbis virus: synthesis and organization of proteins in cells infected with wild-type and maturation-defective mutants. J. Virol. **22:**662–678.
37. **Strauss, J. H., and E. G. Strauss.** 1994. The alphaviruses: gene expression, replication, and evolution. Microbiol. Rev. **58:**491–562.
38. **Suomalainen, M., P. Liljeström, and H. Garoff.** 1992. Spike protein-nucleocapsid interactions drive the budding of alphaviruses. J. Virol. **66:**4737–4747.
39. **Syväoja, P., J. Peränen, M. Suomalainen, S. Keränen, and L. Kääriäinen.** 1990. A single amino acid change in E3 of ts1 mutant inhibits the intracellular transport of SFV envelope protein complex. Virology **179:**658–666.
40. **Wahlberg, J. M., W. A. M. Boere, and H. Garoff.** 1989. The heterodimeric association between the membrane proteins of Semliki Forest virus changes its sensitivity to low pH during virus maturation. J. Virol. **63:**4991–4997.
41. **White, J. M.** 1990. Viral and cellular membrane fusion proteins. Annu. Rev. Physiol. **52:**675–697.
42. **Wiley, D. C., and J. J. Skehel.** 1987. The structure and function of the hemagglutinin membrane glycoprotein of influenza virus. Annu. Rev. Biochem. **56:**365–394.
43. **Zhao, H., and H. Garoff.** 1992. Role of cell surface spikes in alphavirus budding. J. Virol. **66:**7089–7095.
44. **Zhao, H., B. Lindqvist, H. Garoff, C.-H. von Bonsdorff, and P. Liljeström.** 1994. A tyrosine-based motif in the cytoplasmic domain of the alphavirus envelope protein is essential for budding. EMBO J. **13:**4204–4211.
45. **Ziemiecki, A., and H. Garoff.** 1978. Subunit composition of the membrane glycoprotein complex of Semliki Forest virus. J. Mol. Biol. **122:**259–269.
46. **Ziemiecki, A., H. Garoff, and K. Simons.** 1980. Formation of the Semliki Forest virus membrane glycoprotein complexes in the infected cell. J. Gen. Virol. **50:**111–123.